Journal of Organometallic Chemistry, 475 (1994) 127–137

Titanium-magnesium complexes containing perpendicularly bridging bis(trimethylsilyl)acetylene ligands

V. Varga and K. Mach

J. Heyrovský Institute of Physical Chemistry, Academy of Sciences of the Czech Republic, Dolejškova 3, 182 23 Praha 8 (Czech Republic)

G. Schmid and U. Thewalt

Sektion Röntgen- und Elektronenbeugung, Universität Ulm, D-89069 Ulm (Germany)

(Received January 18, 1994)

Abstract

Binuclear complexes $[Cp'Ti][\mu\text{-}\eta^2\text{: }\eta^2\text{-}C_2(SiMe_3)_2]_2[Cp'Mg]$, where $C_2(SiMe_3)_2$ is bis(trimethylsilyl)acetylene (BTMSA) and $Cp' = \eta^5\text{-}C_5H_5$ (**1C**) or $\eta^5\text{-}C_5H_4Me$ (**2C**), and trinuclear complexes $[Cp'Ti][\mu\text{-}\eta^2\text{: }\eta^2\text{-}C_2(SiMe_3)_2]_2[Mg(\mu\text{-}Cl)_2][Cp'Mg(THF)]$ with $Cp' = \eta^5\text{-}C_5H_4Me$ (**2D**) and $\eta^5\text{-}C_5H_3Me_2$ (1,3-dimethyl) (**3D**), were obtained from Cp'_2TiCl_2/Mg(excess)/BTMSA(excess)/THF systems either pure (for **1C** and **3D**) or as a mixture (for **2C** and **2D**). Binuclear complexes **1C**, **2C** and **3C** ($Cp' = \eta^5\text{-}C_5H_3Me_2$; 1,3-dimethyl) were also obtained by reacting the corresponding titanocene-BTMSA complexes $Cp'_2Ti[\eta^2\text{-}C_2(SiMe_3)_2]$ (**1B–3B**) with magnesium and BTMSA in THF. The X-ray crystal structures of compounds **1C**, **2C**, **2D** and **3D** showed a short Ti–Mg distance (2.755(4)–2.768(2) Å) and a considerable sp^2 hybridization at the acetylenic carbon atoms as follows from the C–C–Si angles 137.4(5)–139.9(16)°. Compound **3C** was characterized by spectroscopic data which indicate that its structure is analogous to that of **1C** and **2C**.

Key words: Titanium; Magnesium; Bis(trimethylsilyl)acetylene; Bridging ligand; X-ray structure

1. Introduction

Complexes containing one or two perpendicularly bridging acetylene ligands are known for most of the transition metal elements. Their syntheses and structures have been recently reviewed as a special class of μ-hydrocarbon-bridged transition metal complexes [1]. The electronic structures of transition metal complexes with parallel and perpendicular acetylene bridges were discussed in an earlier comprehensive review [2]. The synthesis and crystal structure of the first titanium complex of this class of complexes, $[(\eta^5\text{-}C_5H_5)Ti][\mu\text{-}\eta^2\text{: }\eta^2\text{-}C_2(SiMe_3)_2]_2[(\eta^5\text{-}C_5H_5)Mg]$ (**1C**), has been reported only recently by us in a preliminary communication [3]. Complex **1C** was the only product of the reduction of $(\eta^5\text{-}C_5H_5)_2TiCl_2$ by magnesium in THF in the presence of bis(trimethylsilyl)acetylene (BTMSA), at the molar ratios Ti: Mg: BTMSA = 1 : 2 : 2. The titanocene-BTMSA complex $(\eta^5\text{-}C_5H_5)_2Ti[\eta^2\text{-}C_2(SiMe_3)_2]$ was found to be an intermediate and the further reaction of the isolated complex with Mg and BTMSA afforded **1C** quantitatively.

Since the electron donation effect of Me groups at cyclopentadienyl ligands strongly changes the reactivity of various titanocene derivatives [4–6] the investigation of the formation of complexes analogous to **1C** has been extended to the whole series of $(\eta^5\text{-}C_5H_{5-n}Me_n)_2TiCl_2$ ($n = 0$–5) compounds as starting materials. Here we report the preparative details of obtaining such complexes and their X-ray crystal structures and other spectroscopic characteristics.

2. Experimental details

All-sealed glass devices equipped with magnetically breakable seals were used to handle the reaction components, solvents and products using a high-vacuum

Correspondence to: Dr. K. Mach or Prof. U. Thewalt.

0022-328X/94/$7.00
SSDI 0022-328X(94)24516-L

line operated with metal valves. NMR and ESR sample tubes and quartz optical cells were sealed after filling. Filling of infrared cuvettes, preparation of KBr pellets, and adjustment of single crystals into capillaries for the X-ray analysis were carried out in an atmosphere of purified nitrogen.

2.1. Chemicals

The solvents (tetrahydrofuran (THF), hexane, toluene and C_6D_6 (Fluka)) were purified by standard methods, dried by refluxing over $LiAlH_4$ and stored in ampoules attached to a vacuum line as solutions of dimeric titanocene $[(\eta^5\text{-}C_5H_5)TiH]_2(\eta^5\text{:}\ \eta^5\text{-}C_{10}H_8)$ [7]. Bis(trimethylsilyl)acetylene (BTMSA) (Fluka) was degassed, purified by dimeric titanocene as above and distributed into ampoules by distillation on a vacuum line. Magnesium turnings (Fluka, purum for Grignard reactions) were used in a large excess for the preparation of **1C** and the unreacted, activated metal was used for the preparation of the other compounds. All the mentioned reactions also proceeded with the unactivated Mg but irreproducible induction periods occurred. Cyclopentadiene and methylcyclopentadiene dimers (both Fluka) were monomerized by distillation at normal pressure. Titanocene dichlorides $(\eta^5\text{-}C_5H_5)_2TiCl_2$ (**1A**) and $(\eta^5\text{-}C_5H_4Me)_2TiCl_2$ (**2A**) were prepared by the usual procedure from $TiCl_4$ and 2 equiv of cyclopentadienyllithium and methylcyclopentadienyllithium in tetrahydrofuran (THF) [8]. 1,3-Dimethylcyclopentadiene was obtained from 3-methyl-2-cyclopentenone (Fluka) by the reaction with 1.4 equiv of MeMgI in diethyl ether followed by hydrolysis and dehydration induced by iodine. Distillation of the freshly prepared crude product at 760 Torr (106–118°C) afforded a mixture of 1,3-dimethylcyclopentadienes in 43% yield. Bis(1,3-dimethylcyclopentadienyl)titanium dichloride $(\eta^5\text{-}C_5H_3Me_2)_2TiCl_2$ (**3A**) was obtained from $TiCl_3$ and 2 equiv of $(C_5H_3Me_2)Li$ in THF using a final oxidation by aqueous HCl. Red thin-needle crystals were obtained by subsequent crystallization from a $CHCl_3$/methanol mixture and from toluene. Yield 55%. $(\eta^5\text{-}C_5H_3Me_2)_2TiCl_2$ (**3A**): ^1H NMR ($CDCl_3$): δ 2.187 (s, 6 H, 2 × Me); 6.018 (d, 2H, J = 2.3 Hz, H-4, H-5); 6.246 (t, 1 H, J = 2.3 Hz, H-2). ^{13}C NMR ($CDCl_3$): δ 16.97 (q, 2C); 116.10 (d, 2C); 125.83 (d, 1C); 134.09 (s, 2C). ^1H NMR (C_6D_6): δ 1.974 (s, 6H, 2 × Me); 5.378 (d, 2 H, J = 2.4 Hz, H-4, H-5); 5.968 (t, 1 H, J = 2.4 Hz, H-2). ^{13}C NMR (C_6D_6): δ 16.93 (q, 2C); 115.26 (d, 2C); 126.09 (d, 1C); 133.45 (s, 2C). MS (direct inlet, 75 eV, 110–125°C; m/e(%)): 306($M_i^{+\bullet}$, 16.4), 304($M^{+\bullet}$, 23.5), 269(12.0) 268(16.0), 233(21.1), 232(36.6), 213(45.1), 211(58.2), 176(20.2), 175(40.0), 93(100.0). No impurity was detected.

2.2. Preparation of $Cp'_2Ti[\eta^2\text{-}C_2(SiMe_3)_2]$ complexes 1B–3B

Cp'_2TiCl_2 (2 mmol) and Mg (0.0486 g, 2 mmol) were weighed into an ampoule equipped with a teflon coated magnetic stirrer. The ampoule was evacuated and THF (30 ml) and BTMSA (0.6 ml, 2.5 mmol) were distilled in, on a vacuum line. The mixture was frozen by liquid nitrogen and the ampoule was sealed off. After stirring at room temperature for two days all magnesium had dissolved and a clear yellow solution was obtained. THF was evaporated on a vacuum line with heating up to 60°C and the yellow residue was extracted by hexane. Compounds **1B–3B** were obtained in almost quantitative yields. Only the data which are relevant for comparison with those of the title complexes are listed.

$(\eta^5\text{-}C_5H_5)_2Ti[\eta^2\text{-}C_2(SiMe_3)_2]$ (**1B**). ^1H NMR (C_6D_6): δ −0.333 (s, 18H, 2 × $SiMe_3$); 6.410 (s, 10H). ^{13}C NMR (C_6D_6): δ 0.59 (q, 6C, 2 × $SiMe_3$); 117.82 (d, 10C); 244.77 (s, 2C, C≡C). UV-Vis (λ_{max}, nm, hexane): 1060br 360sh < 272sh nm. IR (hexane, cm^{-1}): 1720m, sh, 1682s, 1641m, sh, 1583w, sh. The NMR and IR data agree with the literature [9].

$(\eta^5\text{-}C_5H_4Me)_2Ti[\eta^2\text{-}C_2(SiMe_3)_2]$ (**2B**). ^1H NMR (C_6D_6): δ −0.270 (s, 18H, 2 × $SiMe_3$); 2.095 (s, 6H, 2 × Me); 5.395 (t, 4H, 2 × H-3,4, J = 2.7 Hz); 6.442 (t, 4H, 2 × C-2,5, J = 2.7 Hz) ^{13}C NMR (C_6D_6): δ 1.18 (q, 6C); 16.98 (q, 2C); 114.08 (d, 4C, 2 × C-2,5); 115.90 (d, 4C, 2 × C-3,4); 130.92 (s, 2C, 2 × C-1); 245.28 (s, 2C, C≡C). UV-Vis (λ_{max}, hexane): 990br 350sh < 272sh nm. IR (hexane, cm^{-1}): 1720m, sh, 1672s, 1636s, sh, 1581m, sh.

$(\eta^5\text{-}C_5H_3Me_2)_2Ti[\eta^2\text{-}C_2(SiMe_3)_2]$ (**3B**). ^1H NMR (C_6D_6): δ −0.228 (s, 18H, 2 × $SiMe_3$); 1.606 (s, 12H, 4 × Me); 5.735 (d, 4H, 2 × H-4,5, J = 2.4 Hz); 6.530 (t, 2 H 2 × H-2, J = 2.4 Hz). ^{13}C NMR (C_6D_6): δ 1.54 (q, 6C); 15.90 (q, 4C, Me-1, 3); 115.54 (d, 4C, 2 × C-4, 5); 116.13 (d, 2C, 2 × C-2); 128.17 (s, 4C, 2 × C-1, 3); 245.54 (s, 2C, C≡C). UV-Vis (λ_{max}, hexane): 985br 352sh < 270sh nm. IR (hexane, cm^{-1}): 1720w, sh, 1670s, 1635s, 1603m, sh.

2.3. Preparation of complexes 1C, 2C, 2D and 3D from the Cp'_2TiCl_2 compounds

In a typical procedure Cp'_2TiCl_2 (2 mmol) was weighed into an ampoule equipped with two breakable seals and a teflon coated magnetic stirrer. The ampoule was evacuated on a vacuum line and BTMSA (1.4 ml, 6 mmol) and THF 30 ml were distilled in. After cooling by liquid nitrogen the ampoule was sealed off and activated Mg turnings (*ca.* 0.5 g, about 20 mmol) were added from a side-arm ampoule. The reaction mixture was stirred at 60°C typically for two days. During this time the colour changed from red via yellow to green. THF was evaporated *in vacuo* finally

at 60°C and the solid residue changed its colour to red. The solid was extracted with hexane to leave a white powder of $MgCl_2$. Crystalline **1C** was obtained by crystallization from hot hexane in 93% yield (1.0 g).

$[(\eta^5\text{-}C_5H_5)Ti][\mu\text{-}\eta^2 : \eta^2\text{-}C_2(SiMe_3)_2]_2[(\eta^5\text{-}C_5H_5)\text{-}Mg]$ (**1C**). ^1H NMR (C_6D_6): δ 0.132 (s, 36H, $4 \times SiMe_3$); 5.983 (s, 5H); 6.402 (s, 5H); ^{13}C NMR (C_6D_6): δ 1.43 (q, 12C); 107.87 (d, 5C); 110.62 (d, 5C); 269.07 (s, 4C); UV-Vis (hexane, red): 305sh, 377vs, 440sh, 525m nm; (THF, green): 360s, 480sh, 620m nm. IR (KBr pellet, cm^{-1}): 3098vw, 2955m, 2897m, 1663vw, 1622vw, 1524m, 1478s, 1402w, 1242s, 1115vw, 1011m, 860sh, 839vs, 775s, 750s, 691w, 640m, 625w, 505vw, 463m, 419w; (hexane, cm^{-1}): the same within ± 3 cm^{-1} except that two bands at 475w and 463w were resolved. MS (direct inlet, 135–155°C; *m/e* (%)): 542 ($M^{+\bullet}$, 0.5), 372 (1.0), 348 (6.7), 283 (1.5), 281 (2.5), 277 (1.5), 275 (3.3) 243 (0.6), 241 (1.3), 202 (Cp_2TiMg, 4.8), 178 (Cp_2Ti, 100), 155 (93), 113 (CpTi, 10), 89 (CpMg, 4.5), 73 (73), 65 (11). Elemental analysis: 542.1992, error $+1.4 \times 10^{-3}$ for $C_{26}H_{46}MgSi_4Ti$; 202.0115, error -3×10^{-4} for $C_{10}H_{10}MgTi$; EDX (Kα) Mg, Si, Ti (approx. ratio Ti: Mg = 1 : 1).

A mixture of **2C** and **2D** was obtained by an analogous procedure. The products were separated as follows. The more soluble fraction, containing **2C**, was extracted first. Then the much less soluble **2D** was separated from a white powder of $MgCl_2$ by repeated extraction until the residue remained white. Two hexane washings of the collected **2D** were discarded to remove **2C** and the rest was crystallized from the hot solution. Crystalline **2C** was obtained in a yield of 57% (0.65 g). Crystalline **2D** was collected in 28% yield (0.37 g).

$[(\eta^5\text{-}C_5H_4Me)Ti][\mu\text{-}\eta^2 : \eta^2\text{-}C_2(SiMe_3)_2]_2[(\eta^5\text{-}C_5H_4\text{-}Me)Mg]$ (**2C**). ^1H NMR (C_6D_6): δ 0.179 (s, 36H, $4 \times SiMe_3$); 1.739 (s, 6H, Me); 2.338 (s, 6H, Me); 5.748 (t, 2H, $J = 2.7$ Hz); 5.951 (t, 2H, $J = 2.7$ Hz); 6.115 (t, 2H, $J = 2.7$ Hz); 6.328 (t, 2H, $J = 2.7$ Hz); ^{13}C NMR (C_6D_6): δ 1.74 (q, 12C); 15.22 (q, 2C); 106.32 (d, 2C); 108.69 (d, 2C); 108.77 (d, 2C); 111.05 (d, 2C); 118.73 (s, 1C); 124.30 (s, 1C); 269.54 (s, 4C). UV-Vis (hexane, red): 305sh, 378s, 440sh, 525m nm; (THF, green): 370s, 470sh, 620m nm, IR (hexane, cm^{-1}): 1510w, 1400vw, 1250sh, 1243s, 1074vw, 1042w, 1028w, 932w, 861s, 844vs, 815m, 784w, 766sh, 756sh, 746s, 687w, 640w, 621w, 473m, 461w. MS (direct inlet, 185°C; *m/e* (%)): 570 (M^+, not seen), 400 ($Cp'_2TiMg \cdot BTMSA$; 0.6), 376 ($Cp'_2Ti \cdot BTMSA$; 2.1), 230 (Cp'_2TiMg; 2.4), 206 (Cp'_2Ti; 86), 170 (BTMSA; 7), 155 (BTMSA-Me; 100), 127 (Cp'Ti; 6), 103 (Cp'Mg; 6); EDX (Kα) Mg, Si; Ti (approx. ratio Ti : Mg = 1 : 1).

$[(\eta^5\text{-}C_5H_4Me)Ti][\mu\text{-}\eta^2 : \eta^2\text{-}C_2(SiMe_3)_2]_2[Mg(\mu\text{-}Cl)_2][(\eta^5\text{-}C_5H_4Me)Mg(THF)]$ (**2D**). Its structure was determined by X-ray crystal analysis (*vide infra*). The vibrations of the coordinated THF molecule in **2D** and **3D** are probably hidden in strong absorption bands of the trimethylsilyl group in the region 700–900 cm^{-1}. The bands at 1063 and 907 cm^{-1} in **3D** may be partly due to a trace of free THF (THF in toluene absorbs at 1061 and 916 cm^{-1}). Compound **2D** appeared to be unstable in aromatic solvents, slowly separating a white precipitate of $MgCl_2$ and producing **2C**. This circumstance precluded the obtaining of NMR spectra in C_6D_6). IR (KBr pellet, cm^{-1}): 3084vw, 2955s, 2897m, 1516m, 1472s, 1402vw, 1348vw, 1242s, 1062vw, 1035w, 1022m, 934vw, 862sh, 839vs, 815sh, 784sh, 758s, 691w, 642w, 623w, 469m; EDX (Kα) Mg, Si, Cl, Ti, (approx. ratio Ti: Mg = 1 : 2)

Compound **3D** was obtained as the only product by repeated extraction with hexane of the solid reaction product in the amount of 1.17 g (85%). The white remainder was negligible in this case. The first two hexane washings of the collected **3D** were discarded to remove eventual traces of **3C**. Compound **3D** is stable in hexane solution, but in toluene it partly liberated $MgCl_2$ after one month. Its NMR spectra were measured within 6 h after dissolving in C_6D_6 and the spectra obtained differed from those of **3C** (*vide infra*) and clearly indicated the presence of the coordinated THF molecule.

$[(\eta^5\text{-}C_5H_3Me_2)Ti][\mu\text{-}\eta^2 : \eta^2\text{-}C_2(SiMe_3)_2]_2[Mg(\mu\text{-}Cl)_2][(\eta^5\text{-}C_5H_3Me_2)Mg(THF)]$ (**3D**). ^1H NMR (C_6D_6): δ 0.309 (s, 36H, $4 \times SiMe_3$); 1.205 (m, 4H, $-CH_2$ of THF); 1.905 (s, 6H, Me); 2.429 (s, 6H, Me); 3.426 (m, 4H, $-CH_2$ of THF); 5.893 (s, 3H, Cp); 5.990 (s, 3H, Cp). ^{13}C NMR (C_6D_6): δ 1.84 (q, 12C); 15.33 (q, 2C); 15.71 (q, 2C); 24.95 (t, 2C, THF); 69.33 (t, 2C, THF); 103.98 (d, 2C); 106.30 (d, 1C); 107.79 (d, 2C); 112.17 (d, 1C); 117.53 (s, 2C); 122.34 (s, 2C); 273.34 (s, 4C). Accidental degeneracy of chemical shifts for protons at the $C_5H_3Me_2$ ring is observed at variance with chemical shifts for the carbon atoms. UV-Vis (C_6D_6, red): 375s, 440sh, 525m nm; (THF, green): 370s, 470sh, 620m nm. IR (toluene, cm^{-1}): 1242s, 1063m, THF?, 1015w, 907m, THF?, 842vs, 751m, 646m, 621w, 491w, 473w; EDX (Kα) Mg, Si, Cl, Ti (approx. ratio Ti : Mg = 1 : 2).

2.4. Preparation of 1C–3C from $Cp'_2Ti[\eta^2\text{-}C_2(SiMe_3)_2]$ (1B–3B) by the reaction with Mg and BTMSA

Complexes **1B–3B** as prepared above (*ca.* 2 mmol) were dissolved in THF under vacuum conditions, activated Mg turnings (*ca.* 0.5 g) were added and BTMSA (0.7 ml, 3 mmol) was distilled in. After cooling by liquid nitrogen the ampoule was sealed off. In the case of **1B** and **2B** the reaction mixture was stirred at 60°C for two days, however, the change of colour from yellow to green had already occurred after several hours. The

workup described above afforded **1C** and **2C** in 95% yields. The reaction mixture containing **3B** was stirred at 60°C to give a yellow-green solution. THF was evaporated and the residue was extracted by hexane. The product was purified from the more soluble unreacted **3B** by extraction of the latter with a condensing hexane vapour. This procedure was repeated to afford **3C** as a red crystalline material containing only a small amount of **3B** as detected by ^{1}H NMR and MS measurements. The identification of the product as **3C** was based on ^{1}H and ^{13}C NMR spectra and mass spectra. The yield of crystalline **3C** was 0.18 g (15%). [(η^5-$C_5H_3Me_2$)Ti][μ-η^2 : η^2-$C_2(SiMe_3)_2$]$_2$[(η^5-$C_5H_3Me_2$)-Mg] (**3C**). ^{1}H NMR (C_6D_6): δ 0.232 (s, 36H, 4 × $SiMe_3$); 1.839 (s, 6H, 2 × Me); 2.370 (s, 6H, 2 × Me); 5.688 (t, 1H, 2.5 Hz); 5.807 (d, 2H, J = 2.5 Hz); 5.890 (t, 1H, J = 2.5 Hz); 6.059 (d, 2H, J = 2.5 Hz). ^{13}C NMR (C_6D_6): δ 2.25 (q, 12C); 15.36 (q, 2C); 15.61 (q, 2C); 107.12 (d, 2C); 110.00 (d, 1C); 110.14 (d, 2C); 112.66 (d, 1C); 117.17 (s, 2C); 122.09 (s, 2C); 271.08 (s, 4C, C≡C). The assignment of Me and Cp protons was by a delay-COSY experiment. (Impurity (η^5-$C_5H_3Me_2$)$_2$Ti. BTMSA ^{1}H NMR: δ −0.216 (s), 1.607 (s), 5.746 (d, H-4,5, J = 2.4 Hz), 6.531 (t, H-2, J = 2.4 Hz). UV-Vis (hexane, red): 382s, 520sh, m nm; (THF, green): 372s, 620m nm (the bands of **3B** were observed in low intensity). MS (direct inlet, 150–180°C; m/e (probable composition; %)): 598 (M^+; 0.05), 583 (M − Me; 0.1), 428 (M − BTMSA; 0.9), 404 (M − BTMSA − Mg; 1.2), 258 (M − 2 BTMSA; 2.6); 234 (M − 2 BTMSA − Mg; 100), 170 (BTMSA; 5.5), 155 (BTMSA − Me; 70), 73 ($SiMe_3$; 24). The ions of BTMSA (m/e 170, 155, 73) were detected at temperatures 70–90°C which indicated the presence of **3B**.

The same experiments were carried out with the $Cp'_2Ti[\eta^2$-$C_2(SiMe_3)_2]$(Cp' = C_5Me_5, C_5HMe_4, and $C_5H_2Me_3$) complexes [10], however, they remained unchanged as observed visually and by electronic absorption spectroscopy after heating to 60°C for two weeks. All the compounds were recovered as yellow crystalline materials.

In the absence of BTMSA compounds **1B** and **2B** reacted completely with activated Mg turnings during two days at 60°C to give approximately half yields of **1C** and **2C** compared with the above experiments. The hexane solutions of the products showed in addition to the bands of **1C** and **2C** weak absorption bands at 828 nm [7] and at 835 nm which are characteristic of the presence of trace amounts of the dimeric titanocenes [(η^5-C_5H_5)Ti(μ-H)]$_2$(η^5 : η^5-$C_{10}H_8$) and [(η^5-C_5MeH_4)Ti(μ-H)]$_2$(η^5 : η^5-$C_{10}Me_2H_6$), respectively. The residue after extraction with hexane was completely soluble in toluene, however, its composition was not determined.

2.5. Reactions of 1C

The solution of **1C** in m-xylene (0.1 M) remained stable upon heating to 170°C for 2 h; its red colour and the UV-Vis spectrum did not change. The compound was, however, completely decomposed after heating to 200°C for 2 h. All volatiles including m-xylene were distilled off *in vacuo* and the residue was dissolved in hexane to give a brown solution. Its UV-Vis spectrum showed a continuous absorption increasing in intensity from *ca.* 800 nm to shorter wavelengths. Only a trace of dimeric titanocene was present as indicated by a weak absorption band at 828 nm. The GC analysis of the volatiles showed a mixture of 1,2-bis(trimethylsilyl)-ethane, *cis*- and *trans*-1,2-bis(trimethylsilyl)ethylene and BTMSA.

Addition of diphenylacetylene (0.36 g, 2 mmol) to the solution of **1C** in hexane (0.1 M, 4 ml) did not change the red colour of the solution. A white material slowly precipitated from the solution during three months at room temperature. Heating of an analogous mixture to 100°C for 2 h resulted in the precipitation of a white product in the yield of 0.20 g (55%). The product was identified by MS (direct inlet) and IR (KBr pellet) spectra to be hexaphenylbenzene [11]. The concentration of **1C** in both experiments remained unchanged as indicated by UV-Vis spectra. The separated solutions containing unreacted DPA produced additional hexaphenylbenzene.

2.6. Methods

^{1}H and ^{13}C NMR spectra were measured on a Varian VXR-400 instrument (400 and 100 MHz, respectively) in C_6D_6 at 25°C and were referred to the solvent signal (δ_H 7.15 ppm, δ_C 128.0 ppm). A delayed COSY experiment was used for some methyl signal assignments. NMR tubes were filled under vacuum conditions and were sealed off. Mass spectra were recorded on a JEOL JMS D-100 spectrometer at 75 eV. Samples in sealed capillaries were opened and inserted into the direct inlet under argon. Electronic absorption spectra were measured on a Varian Cary 17 D spectrometer in the range 300–2000 nm in 0.1 and 1.0 cm sealed quartz cells (Hellma). Infrared spectra were measured on a UR 75 (Zeiss, Jena) and on a Mattson Galaxy 2020 spectrometer. Samples in hexane solution, Nujol mull and in KBr pellets were prepared in an atmosphere of purified nitrogen. Electron dispersive X-ray analyses (EDX) were carried out on a Zeiss DSM962 electron microscope equipped with an Edax PV9800 analyser.

2.7. X-ray crystal structure analyses of 2C, 2D and 3D

Crystal fragments of **2C**, **2D** and **3D** were mounted into Lindemann glass capillaries under purified nitrogen in a glovebox. The capillaries were closed with

TABLE 1. Crystallographic data and experimental details for **2C**, **2D**, **3D**

	2C	**2D**	**3D**
(a) *Crystal data*			
Chem. formula	$C_{28}H_{50}MgSi_4Ti$	$C_{32}H_{58}Cl_2Mg_2OSi_4Ti$	$C_{34}H_{62}Cl_2Mg_2OSi_4Ti$
Mol. wt. [g/mol]	571.2	738.6	766.6
Crystal system	triclinic	monoclinic	orthorhombic
Space group	$P\bar{1}$	$P2_1/c$	*Pnma*
a[Å]	9.936(9)	20.165(4)	20.453(3)
b[Å]	10.32(1)	17.640(3)	16.164(4)
c[Å]	11.78(1)	12.372(2)	13.435(3)
α[°]	113.55(7)		
β[°]	99.95(8)	101.33(1)	
γ[°]	118.43(6)		
Z	1	4	4
$D_{calc.}$ [g cm^{-3}]	1.090	1.137	1.146
μ(Mo Kα) [cm^{-1}]	3.72	4.35	4.24
approx. crystal dimensions [mm^3]	0.15 × 0.2 × 0.2	0.1 × 0.3 × 0.7	0.15 × 0.5 × 0.5
(b) *Data collection and refinement*			
$2\theta_{max.}$(°)	40	40	43
unique observed reflections			
total	1600	3725	2622
$F_o > 1\sigma(F_o)$	1442	3125	2307
No. of variables	157	383	212
R	0.096	0.093	0.075
R_w	0.117	0.096	0.080

sealing wax. The X-ray measurements were carried out on a Philips PW1100 four circle diffractometer, using graphite monochromated MoKα radiation (λ = 0.71069 Å) at room temperature. The structure of **2C** was solved by using the statistically weighted tangent formula of MULTAN90 [12], whereas the structures of **2D** and **3D** were solved by iterative symbolic addition (ISA) [12]. Crystallographic data for **2C**, **2D** and **3D** are summarized in Table 1. The structure of **2C** shows the same type of orientation disorder as previously observed for **1C** [3]. Refinement in the space groups $P1$ and $P\bar{1}$ (one molecule of **2C** per unit cell) showed that the latter is the more appropriate space group for **2C**. In this case the molecule has a crystallographic centre of symmetry, which means that the structure is disordered and that the Ti and Mg atom are statistically interchanged. For further refinement the following model was used. Both the Ti and Mg atom and the corresponding atoms in the organic part of **2C** occupy equal positions. Therefore the site occupation factors of Ti and Mg were set to 0.5 and both atoms were given identical coordinates and temperature factors. This model results in a reasonable form of the temperature factors. The present type of disorder is reflected in the relatively high elongation of the thermal ellipsoids of C(4) and C(5) atoms parallel to the Ti(1)–Mg(1) vector. All non-hydrogen atoms in **2C**, **2D** and **3D** were refined with anisotropic temperature factors. Hydrogen atoms were included in calculated positions as contributions to F_c. The PC-ULM-package [12] was used for all calculations. The atomic coordinates of **2C**, **2D** and **3D** are given in Tables 2–4. Selected bond distances and angles for **2C**, **2D** and **3D** are listed in Tables 5–7 [13 *].

TABLE 2. Atomic parameters for **2c** [a]

	x	y	z	U_{eq}
MM'	−0.1381(3)	−0.1757(3)	−0.0700(2)	0.040(1)
C(10)	−0.4354(12)	−0.4001(12)	−0.1576(12)	0.061(6)
C(100)	−0.5572(16)	−0.3558(18)	−0.1376(16)	0.091(9)
C(11)	−0.3423(14)	−0.4152(12)	−0.0680(12)	0.064(6)
C(12)	−0.2463(15)	−0.4618(13)	−0.1241(16)	0.078(9)
C(13)	−0.2785(14)	−0.4780(14)	−0.2503(13)	0.068(7)
C(14)	−0.3942(13)	−0.4359(12)	−0.2731(11)	0.059(6)
C(110)	0.0878(14)	−0.0172(14)	0.1341(10)	0.058(6)
Si(2)	−0.0765(3)	0.1129(4)	0.2945(3)	0.050(2)
C(111)	0.4076(17)	0.1308(19)	0.3745(13)	0.089(9)
C(112)	0.2792(14)	−0.1696(16)	0.0900(12)	0.065(7)
C(113)	0.0804(17)	−0.2277(16)	0.2573(13)	0.078(8)
C(120)	−0.0051(14)	0.0454(14)	0.1591(10)	0.053(6)
Si(1)	0.2112(4)	−0.0688(4)	0.2149(3)	0.050(2)
C(121)	−0.2326(16)	−0.0775(17)	0.2978(14)	0.080(8)
C(122)	0.1133(15)	0.2808(19)	0.4658(11)	0.088(8)
C(123)	−0.1808(19)	0.2086(21)	0.2573(16)	0.105(11)

[a] MM' denotes the position occupied 50% by Ti(1) and 50% by Mg(1) because of the assumed disorder (see Fig. 1).

* Reference number with asterisk indicates a note in the list of references.

3. Results and discussion

The Cp'_2TiCl_2/Mg(excess)/BTMSA(excess)/THF systems, where $Cp' = \eta^5$-C_5H_5 (**1A**), η^5-C_5H_4Me (**2A**), and η^5-$C_5H_3Me_2$ (1,3-dimethyl) (**3A**), when stirred at 60°C, rapidly yielded yellow solutions which then slowly changed to a green colour. The stable yellow solutions were obtained from the same systems at the $Cp'C_2Ti$-Cl_2/Mg molar ratio equal to 1 and the products were identified as the $Cp'_2Ti(\eta^2$-$C_2(SiMe_3)_2]$ (**1B–3B**) complexes. Their further conversion in the presence of magnesium was followed by electronic absorption spectra showing a decrease in the intensity of a broad band at 900–1000 nm belonging to the BTMSA complexes.

TABLE 3. Atomic parameters of **2D**

	x	y	z	U_{eq}
Ti(1)	0.3545(1)	−0.0463(1)	0.2505(1)	0.053(1)
C(11)	0.4277(8)	−0.1421(10)	0.2015(17)	0.147(5)
C(111)	0.4057(10)	−0.1894(12)	0.0980(18)	0.255(5)
C(12)	0.4626(6)	−0.0760(9)	0.2141(14)	0.124(5)
C(13)	0.4711(7)	−0.0574(14)	0.3244(18)	0.184(5)
C(14)	0.4417(10)	−0.1034(14)	0.3708(16)	0.210(5)
C(15)	0.4127(8)	−0.1629(9)	0.3089(22)	0.211(5)
Mg(1)	0.2370(2)	0.0384(2)	0.2066(3)	0.059(2)
Cl(1)	0.1978(1)	0.1477(2)	0.2810(2)	0.075(2)
Cl(2)	0.1349(1)	0.0238(2)	0.0787(3)	0.087(2)
Mg(2)	0.0958(2)	0.1451(2)	0.1374(3)	0.076(2)
C(21)	0.1007(9)	0.2738(9)	0.0792(15)	0.137(5)
C(211)	0.1387(16)	0.3311(10)	0.1520(19)	0.325(5)
C(22)	0.0403(12)	0.2622(10)	0.0926(16)	0.171(5)
C(23)	0.0119(8)	0.2138(13)	0.0195(22)	0.215(5)
C(24)	0.0578(17)	0.1875(11)	−0.0430(15)	0.253(5)
C(25)	0.1122(10)	0.2284(11)	−0.0000(16)	0.166(5)
O(3)	0.0335(3)	0.1003(4)	0.2315(6)	0.083(4)
C(31)	−0.0204(7)	0.0481(10)	0.1862(13)	0.154(5)
C(32)	−0.0583(10)	0.0390(12)	0.2684(18)	0.218(5)
C(33)	−0.0330(10)	0.0885(13)	0.3604(16)	0.226(5)
C(34)	0.0279(8)	0.1231(11)	0.3367(11)	0.158(5)
C(4)	0.2607(4)	−0.0874(5)	0.2724(7)	0.048(4)
Si(4)	0.1983(2)	−0.1646(2)	0.2391(3)	0.080(2)
C(41)	0.2371(9)	−0.2510(7)	0.3167(12)	0.150(5)
C(42)	0.1140(6)	−0.1439(9)	0.2789(12)	0.144(5)
C(43)	0.1840(6)	−0.1844(7)	0.0896(9)	0.092(5)
C(5)	0.2859(5)	−0.0429(5)	0.3570(7)	0.049(4)
Si(5)	0.2767(2)	−0.0289(2)	0.5028(2)	0.080(2)
C(51)	0.3158(11)	−0.1104(8)	0.5812(10)	0.204(5)
C(52)	0.1882(8)	−0.0226(12)	0.5161(12)	0.198(5)
C(53)	0.3211(8)	0.0580(8)	0.5621(10)	0.133(5)
C(6)	0.3263(4)	0.0236(5)	0.1130(8)	0.051(4)
Si(6)	0.3128(2)	0.0343(2)	−0.0400(2)	0.076(2)
C(61)	0.3945(7)	0.0332(13)	−0.0802(11)	0.203(5)
C(62)	0.2688(9)	0.1223(9)	−0.0889(11)	0.174(5)
C(63)	0.2581(8)	−0.0406(9)	−0.1067(10)	0.148(5)
C(7)	0.3543(4)	0.0659(5)	0.1984(8)	0.057(4)
Si(7)	0.3974(2)	0.1595(2)	0.2296(3)	0.090(2)
C(71)	0.4791(8)	0.1511(10)	0.1844(17)	0.229(5)
C(72)	0.4103(8)	0.1783(8)	0.3778(10)	0.140(5)
C(73)	0.3480(10)	0.2400(7)	0.1622(13)	0.180(5)

TABLE 4. Atomic parameters for **3D**

	x	y	z	U_{eq}
Ti(1)	0.2440(1)	0.2500	0.1598(1)	0.046(1)
C(11)	0.2915(5)	0.1798(5)	0.2984(5)	0.080(6)
C(111)	0.3159(7)	0.0911(6)	0.2966(7)	0.133(9)
C(12)	0.3314(6)	0.2500	0.2829(7)	0.070(7)
C(13)	0.2290(5)	0.2039(6)	0.3263(5)	0.092(7)
Mg(1)	0.2046(1)	0.2500	−0.0373(2)	0.047(2)
Cl(1)	0.1822(1)	0.3549(1)	−0.1530(1)	0.058(1)
Mg(2)	0.1534(1)	0.2500	−0.2760(2)	0.052(2)
C(21)	0.0572(4)	0.1788(5)	−0.3294(7)	0.079(6)
C(211)	0.0440(4)	0.0901(5)	−0.2979(9)	0.114(8)
C(22)	0.0359(5)	0.2500	−0.2703(10)	0.072(8)
C(23)	0.0909(4)	0.2063(5)	−0.4157(8)	0.099(7)
O(3)	0.2412(3)	0.2500	−0.3451(4)	0.058(4)
C(31)	0.2695(4)	0.1780(5)	−0.3946(6)	0.071(5)
C(32)	0.3366(4)	0.2016(5)	−0.4245(7)	0.087(6)
C(4)	0.3027(3)	0.2088(3)	0.0426(4)	0.040(3)
Si(4)	0.3537(1)	0.1243(1)	−0.0119(1)	0.054(1)
C(41)	0.4347(3)	0.1268(5)	0.0518(6)	0.081(5)
C(42)	0.3663(4)	0.1359(6)	−0.1466(5)	0.091(6)
C(43)	0.3124(4)	0.0224(4)	0.0101(7)	0.081(6)
C(5)	0.1515(3)	0.2086(4)	0.1134(4)	0.048(4)
Si(5)	0.0908(1)	0.1237(1)	0.1185(2)	0.071(1)
C(51)	0.0548(7)	0.1244(8)	0.2458(10)	0.188(12)
C(52)	0.0244(5)	0.1325(7)	0.0255(12)	0.165(12)
C(53)	0.1305(4)	0.0236(5)	0.0975(9)	0.110(8)

In all cases green solutions were finally obtained showing practically the same electronic absorption spectrum. THF was then evaporated *in vacuo* and the residue changed its colour to dark red. After further evacuation to 10^{-3} Torr at 60°C, the residue was extracted with n-hexane. The system based on **1A** yielded the well-soluble compound **1C** [3] and colourless $MgCl_2$ remained. The extraction of the residue in the **2A**-based system afforded a fraction with a more soluble compound **2C** and a less soluble compound **2D**. The system based on **3A** yielded only **3D**, which has a low solubility. The X-ray crystal structure determination revealed

TABLE 5. Selected bond distances [Å] and angles [°] for **2C**

Bond distances			
MM′–CE(Cp ring)	2.044(14)	C(110)–C(120)	1.366(19)
MM′–C(Cp)(av.)	2.371(18)	C(110)–Si(1)	1.822(14)
MM′–C(110)	2.234(14)	C(120)–Si(2)	1.873(14)
MM′–C(110)′	2.273(14)		
MM′–C(120)	2.284(13)		
MM′–C(120)′	2.181(13)		
MM′–M′M	2.755(4)		
Valence angles			
MM′–C(110)–M′M	75.3(4)		
MM′–C(120)–M′M	76.2(4)		
Si(1)–C(110)–C(120)	139.8(11)		
Si(2)–C(120)–C(110)	137.8(11)		

MM′ denotes the position occupied 50% by Ti(1) and 50% by Mg(1) because of the assumed disorder.

TABLE 6. Selected bond distances [Å] and angles [°] for **2D**

Bond distances			
Ti(1)–CE(Cp ring)	2.068(19)	Mg(1)–Cl(1)	2.340(4)
Ti(1)–C(Cp)(av.)	2.367(38)	Mg(1)–Cl(2)	2.352(4)
Ti(1)–C(4)	2.094(9)	Mg(1)–C(4)	2.380(9)
Ti(1)–C(5)	2.090(9)	Mg(1)–C(5)	2.402(10)
Ti(1)–C(6)	2.088(9)	Mg(1)–C(6)	2.338(10)
Ti(1)–C(7)	2.080(10)	Mg(1)–C(7)	2.435(10)
C(4)–C(5)	1.328(13)	C(4)–Si(4)	1.845(10)
C(6)–C(7)	1.326(13)	C(5)–Si(5)	1.866(10)
Mg(2)–CE(Cp ring)	2.063(21)	C(6)–Si(6)	1.868(10)
Mg(2)–C(Cp)(av.)	2.351(24)	C(7)–Si(7)	1.871(10)
Mg(2)–O(3)	2.033(8)	Mg(2)–Cl(1)	2.440(5)
Ti(1)–Mg(1)	2.763(4)	Mg(2)–Cl(2)	2.439(5)
Bond angles			
Ti(1)–C(4)–Mg(1)	76.0(3)	Si(4)–C(4)–C(5)	138.8(7)
Ti(1)–C(5)–Mg(1)	75.6(3)	Si(5)–C(5)–C(4)	138.1(7)
Ti(1)–C(6)–Mg(1)	77.0(3)	Si(6)–C(6)–C(7)	134.9(8)
Ti(1)–C(7)–Mg(1)	75.0(3)	Si(7)–C(7)–C(6)	140.2(8)
Mg(1)–Cl(1)–Mg(2)	90.0(2)	Cl(1)–Mg(1)–Cl(2)	92.1(2)
Mg(1)–Cl(2)–Mg(2)	89.7(2)	Cl(1)–Mg(2)–Cl(2)	87.6(2)
CE(Cp ring)–Mg(2)–O(3)	121.2(3)		
Cl(1)–Mg(2)–CE(Cp ring)	124.3(2)		
Cl(2)–Mg(2)–O(3)	95.9(3)		

that **1C** [3] and **2C** (Fig. 1) are binuclear complexes whereas **2D** and **3D** are trinuclear complexes (Figs. 2 and 3, respectively). The reactions leading to the products can be described by Scheme 1.

The ease of formation of the trinuclear complexes apparently depends on the number of Me groups at the Cp′ rings. The electron donation effect of the Me groups is compensated by insertion of an ionic $MgCl_2$/THF moiety. The intermediacy of the binuclear complexes in the formation of the trinuclear complexes follows from the mechanistic requirement of proximity of Ti and Mg atoms during the Cp′ group transfer from Ti to Mg atom.

Compounds **1C** and **2C** were also obtained by reacting of isolated complexes $Cp'_2Ti[\eta^2\text{-}C_2(SiMe_3)_2]$ (**1B**) and **2B** with Mg in THF in the presence of BTMSA in

TABLE 7. Selected bond distances [Å] and angles [°] for **3D**

Bond distances			
Ti(1)–CE(Cp ring)	2.067(8)	Mg(1)–Cl(1)	2.345(2)
Ti(1)–C(Cp)(av.)	2.402(27)		
Ti(1)–C(4)	2.088(6)	Mg(1)–C(4)	2.370(6)
Ti(1)–C(5)	2.101(6)	Mg(1)–C(5)	2.393(6)
C(4)–C(4)′	1.330(8)	C(4)–Si(4)	1.869(6)
C(5)–C(5)′	1.338(8)	C(5)–Si(5)	1.852(6)
Mg(2)–CE(Cp ring)	2.052(9)		
Mg(2)–C(Cp)(av.)	2.391(12)		
Mg(2)–O(3)	2.021(5)	Mg(2)–Cl(1)	2.440(3)
Ti(1)–Mg(1)	2.768(2)		
Bond angles			
Ti(1)–C(4)–Mg(1)	76.5(2)	Si(4)–C(4)–C(4)′	137.0(4)
Ti(1)–C(5)–Mg(1)	75.7(2)	Si(5)–C(5)–C(5)′	137.8(5)
Mg(1)–Cl(1)–Mg(2)	89.6(1)	Cl(1)–Mg(1)–Cl(1)′	92.6(1)
		Cl(1)–Mg(2)–Cl(1)′	88.0(1)
CE(Cp ring)–Mg(2)–O(3)	122.8(3)		
Cl(1)–Mg(2)–CE(Cp ring)	123.1(3)		
Cl(2)–Mg(2)–O(3)	95.6(1)		

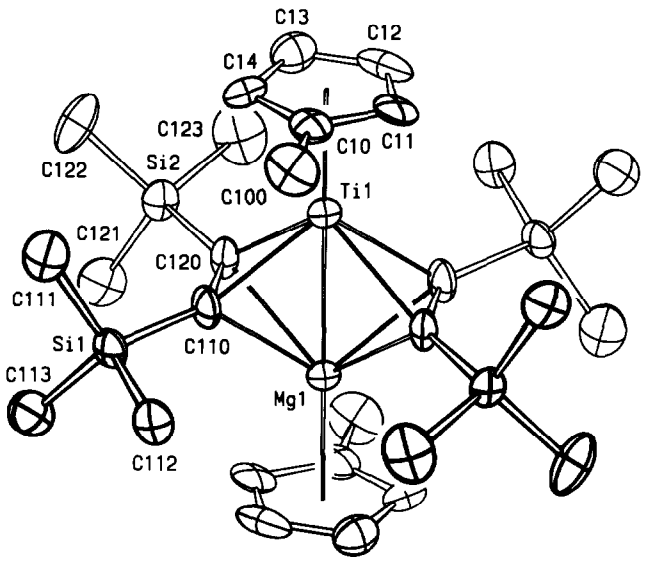

Fig. 1. The molecular structure and atom numbering scheme for **2C**. The Ti(1) and Mg(1) atoms occupy symmetry equivalent positions (see text).

practically quantitative yields. Compound **3C** was obtained only in this way after heating the reaction mixture to 60°C for two weeks. It was obtained in a low yield and had to be separated from unreacted $(\eta^5\text{-}C_5H_3Me_2)_2Ti[\eta^2\text{-}C_2(SiMe_3)_2]$ (**3B**). These results show that the methyl substituents at the Cp′ rings decrease the reactivity of $Cp'_2Ti[\eta^2\text{-}C_2(SiMe_3)_2]$ complexes towards magnesium. The rate of the product formation

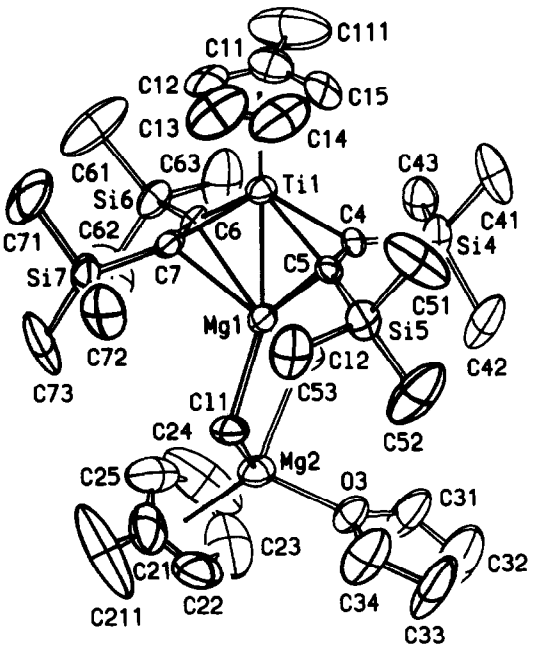

Fig. 2. The molecular structure and atom numbering scheme for **2D**.

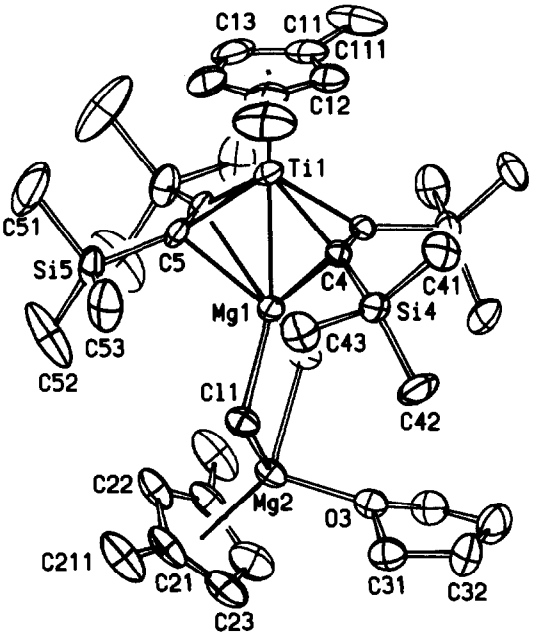

Fig. 3. The molecular structure and atom numbering scheme for **3D**. The atoms C(12), Ti(1), Mg(1), Mg(2), C(22) and O(3) form a mirror plane.

decreased in the order **1B** > **2B** > **3B** and tri-, tetra-, and pentamethylated complexes of this type did not show any reaction with magnesium in the presence of BTMSA, at least under mild conditions (60°C).

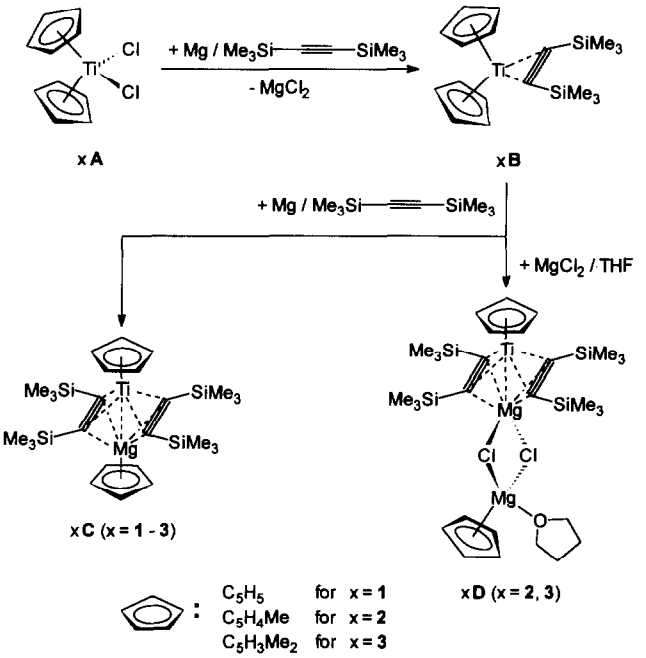

Scheme 1. Formation of complexes of type **C** and **D** via **B** by reduction of $(Cp')_2TiCl_2$ (**A**) with magnesium in THF in the presence of bis(trimethylsilyl)acetylene (BTMSA).

In the absence of an excess of BTMSA, complexes **1C** and **2C** were also formed but in a yield slightly lower than 50% and a mixture of products was obtained. The hexane extracts contained in addition to **1C** or **2C** small amounts of dimeric titanocene ($\eta^5:\eta^5$-fulvalene)(di-μ-hydrido)-bis(η^5-cyclopentadienyltitanium) or its tetramethylated analogue. The extraction of the residue by toluene yielded a brown product, which, however, has not yet been identified. The dimeric titanocenes and the latter products were apparently formed by the decomposition of the **B** type complexes. By this way the BTMSA molecules could be used for the formation of the **C** type complexes. The overall reaction can be tentatively described by eqn. (1).

$$2Cp'_2Ti[\eta^2\text{-}C_2(SiMe_3)_2] + Mg \xrightarrow{THF} [Cp'Ti][\mu\text{-}\eta^2:\eta^2\text{-}C_2(SiMe_3)_2]_2[MgCp'] + [Cp'_2Ti] \quad (1)$$

According to eqn. (1) the attack of Mg on **1B–3B** is essential for the formation of all the products in Scheme 1. The step in which the **1B–3B** complexes are formed can be separated from the formation of the final complexes whose structure depends on the presence of $MgCl_2$ in the system and on the capability of the binuclear complexes **1C–3C** to incorporate it to give the trinuclear complexes **1D–3D**.

The primary green products obtained in THF solutions were not studied by the NMR method because the NMR sample tubes broke upon the cooling by liquid nitrogen which is necessary before sealing off under vacuum conditions. The pyrolysis of THF vapours otherwise produces reactive products which react with low-valent titanium compounds. Since the colour change from green to red was fully reversible upon replacement of THF by hexane or toluene and *vice versa* for all the complexes, we suggest that one molecule of THF is coordinated to the titanium atom in the THF solutions. The strength of this coordination bond is weak because the green-to-red product conversion occurs only on evacuation at ambient temperature. On the other hand, the molecule of THF coordinated to the terminal Mg atom in **2D** or **3D** is not released by evacuation and is not replaced in the hexane or toluene solutions. Its presence as well as that of the $MgCl_2$ moiety does not change noticeably their electronic absorption spectra from those of **1C**, **2C**, and **3C**. This is in line with the virtually identical coordination ligand field at the titanium atom in all these compounds.

3.1. Structure of the products

X-ray structure analyses were carried out for the complexes **1C**, **2C**, **2D** and **3D**. The structure of **1C** has already been discussed in a preliminary communication [3]. The complexes **1C**, **2C**, **2D** and **3D** contain a unit with a Ti and a Mg atom in the apical positions of a nearly rectangular bipyramid whose base is formed by four equivalent acetylenic carbon atoms. In **1C** and **2C** each metal atom is capped by one Cp' ligand (see Fig. 1 for **2C**). In **2D** and **3D** a distorted tetrahedral Cp'Mg(THF) unit is bridged by two Cl atoms to the inner Mg atom (see Figs. 2 and 3, respectively). The structure of **2C** shows the same type of orientation disorder as was observed for **1C**. We assume that the disorder is caused by the similarity of the coordination environments of Ti and Mg atoms. This is in accord with the observation, that the Ti–CE(Cp) and Mg–CE(Cp) distances (CE = centroid of a C_5-ring) are very close to each other (1.98 Å in (η^5-C_5H_5)Ti($AlCl_4$)$_2$ [14], 1.994 Å in (η^5-C_5H_5)(η^7-C_7H_7)Ti [15], 2.01 Å in (η^5-C_5H_5)$TiCl_3$ [16] and 1.981 Å in (η^5-C_5H_5)$_2$Mg [17]). Under the assumption, that $P\bar{1}$ is the most realistic space group for **2C** the Ti and Mg atom are interchanged at the 1:1 ratio. Therefore, the position which is generated by inversion symmetry from the Ti(1)-position will be denoted Mg(1) (see Fig. 1). Complexes of the **D** type show no disorder. The molecule of **3D** contains a crystallographic mirror plane, which contains the atoms

TABLE 8. Comparison of the Cp'Ti(BTMSA)$_2$Mg units in complexes **1C**, **2C**, **2D** and **3D** (distances [Å], angles [°]) [a]

	1C		2C	2D	3D
Ti–CE(Cp ring)	2.08 ± 0.02		2.044(14)	2.068(19)	2.067(8)
Ti–Mg	av. 2.776(2)		2.755(4)	2.763(4)	2.768(2)
Ti–C(ac)		2.04 ± 0.03		av. 2.088(12)	av. 2.095(6)
Mg–C(ac)		2.44 ± 0.03		av. 2.349(19)	av. 2.382(6)
C(ac)–C(ac)	av. 1.319(11)		1.366(19)	av. 1.327(13)	av. 1.334(8)
C(ac)···C(ac)	av. 3.243(27)		3.268(19)	av. 3.240(13)	av. 3.234(8)
C(ac)–Si(ac)	av. 1.859(7)		av. 1.848(26)	av. 1.863(10)	av. 1.861(9)
Si–C(Me)	av. 1.844(22)		av. 1.855(10)	av. 1.842(25)	av. 1.854(15)
C(ac)–C(ac)Si	av. 139.9(16)		av. 138.8(11)	av. 138.0(19)	av. 137.4(5)
Ti–C(ac)–Mg	av. 76.1(4)		av. 75.8(5)	av. 75.9(7)	av. 76.1(4)

[a] Abbreviations: (ac) acetylenic carbon atoms, av. average values, ··· nonbonding distance, ± values are corrected for the disorder.

C(12), Ti(1), Mg(1), Mg(2), C(22) and O(3). Selected bond distances and bond angles of the Cp'Ti(BTMSA)$_2$Mg moiety in **1C**, **2C**, **2D** and **3D** (Table 8) do not show any significant structural differences. The Ti–Mg distance is very constant, within 2.755(4) and 2.768(2) Å. The arguments given earlier for **1C** [3] that it is a complex of Ti^{II} and Mg^{II} with a metal–metal single bond and the Ti^{II} d^2 electrons delocalized in low energy MOs involving π^* orbitals can be applied for all the **C** and **D** type complexes. The Ti–C(ac) bond distances (av. 2.088(12) Å in **2D**, av. 2.095(6) Å in **3D**) are significantly shorter than the Mg–C(ac) bond distances (av. 2.349(19) Å in **2D**, av. 2.382(6) Å in **3D**). In **1C** and **2C**, however, the orientation disorder smears out the difference in the Ti–C(ac) and Mg–C(ac) bond distances. The method of refining a site occupation factor developed for **1C** [3] allows us to evaluate the influence of the disorder on the bond distances involving the metal atoms in **2C**. Least square estimation of a common linear equation system for **1C** and **2C** afforded the Ti–C(ac) distance of 2.04 ± 0.03 Å and the Mg–C(ac) distance of 2.44 ± 0.03 Å, which are virtually the same as those found in **2D** and **3D**. The Ti–C(ac) bond distance is only slightly shorter than the values found for **B** type complexes (η^5-C_5Me_5)$_2$Ti(BTMSA) (av. 2.124(3) Å) [18] and (η^5-C_5HMe_4)$_2$Ti(BTMSA) (2.106(3) Å) [10], where no other metal atom is coordinated to the acetylene. The difference in bonding modes of BTMSA between **B** type complexes and **C** and **D** type complexes is markedly reflected in the shifts of ν(C≡C) frequency and in the values of δ_C for acetylenic carbon atoms (Table 9). The enhanced deshielding in **C** type complexes with respect to **B** type complexes, where BTMSA is considered to be a four-electron donating ligand [21], apparently results from the BTMSA interaction with two metal atoms whereas the back donation can occur for only one of them (Ti^{II}). The structure of **3C**, although not determined by X-ray crystal analysis, was unequivocally established from spectroscopic measurements. The UV-Vis spectra in THF and in hexane were nearly identical with those of all other compounds and IR and ^{1}H and ^{13}C NMR spectra were in agreement with the proposed structure (Table 9). The molecular ion and the fragmentation pattern analogous to **1C** and **2C** were detected in the mass spectrum.

The difference in the bonding properties of Ti and Mg to the BTMSA ligand is also reflected in a displacement of the Si atoms from the bipyramid base plane (max. deviation 0.02 Å in **2D**, 0 Å (mirror) in **3D**) towards the Mg atom by av. 0.27 Å in **2D** and av. 0.35 Å for **3D**. Due to the disorder this displacement was only partially noticed in **1C** (0.1 Å) and could not be observed in **2C** (inversion centre). The BTMSA ligands show the C(ac)–C(ac) bond lengths within the range av. 1.319(11) Å for **1C** and av. 1.366(19) Å for **2C**. The C(ac)–C(ac)–Si angle varies between av. 137.4(5)° for **3D** and 139.9(16)° for **1C**. These values indicate a change in the orbital hybridization from sp in the acetylene to sp^2 in the coordinated ligand. Similar values were also observed in **B** type complexes (η^5-C_5Me_5)$_2$Ti(BTMSA) (1.309 (4) Å, av. 136(1)°) [18] and (η^5-C_5HMe_4)$_2$Ti(BTMSA) (1.303 (5) Å, av. 140(2)°) [10]. No significant interaction can occur between neighbouring carbon atoms of the bipyramid base belonging to different BTMSA ligands (av. distance 3.25(1) Å in **1C**, **2C**, **2D** and **3D**). Differences in the coordination environment of Mg(1) and Mg(2) in **D** type complexes can be seen in a significantly shorter Mg(1)–Cl bond distance (2.346(6) Å in **2D**, 2.345(2) Å in **3D** in comparison to the Mg(2)–Cl bond distance (2.440(5) Å in **2D** and **3D**) and a larger C–Mg–Cl angle for Mg(1) (92.1(2)° in **2D**, 92.6(1)° in **3D**) compared to Mg(2) (87.6(2)° in **2D**, 88.0(1)° in **3D**). The Mg(2)–Cl, Mg(2)–O, Mg(2)–C(Cp) bond distances and the Cl–Mg(2)–Cl, Mg(1)–Cl–Mg(2) bond angles are very similar to those recently found for the Grignard compounds [(η^5-C_5H_5)MgCl(OEt$_2$)]$_2$ and [(η^5-C_5Me_5)MgCl(OEt$_2$)]$_2$ [22]. They are summarized in Table 10. The Mg(1)–Mg(2) nonbonding distance (3.380(4) Å in **2D**, 3.373(2) Å in **3D**) is significantly shorter than in [(η^5-C_5H_5)MgCl(OEt$_2$)]$_2$ (3.43 Å) and [(η^5-C_5Me_5)MgCl(OEt$_2$)]$_2$ (3.52 Å), which is due to extraordinarily short Mg(1)–Cl bond distances in **2D** and **3D**. A negligible deviation of the methyl carbon atoms from the least squares plane of the Cp'-ligands in **2C** (C(111) 0.04 Å),

TABLE 9. Valence ν(C≡C) vibrations and ^{13}C chemical shifts δ_C for the BTMSA complexes

	ν(C≡C) (cm^{-1})	δ_C(C≡C) (ppm)
BTMSA	2108 [a]	113.84 [b]
1B	1682 [c]	244.77
2B	1672 [c]	245.28
3B	1652 [c]	245.54
1C	1524 [d]	269.07
2C	1510 [e]	269.54
2D	1516 [d]	
3C	1510 [e]	271.08
3D	– [f]	273.34

[a] Raman spectrum [19].
[b] Reference [20].
[c] Position of an absorption maximum for a group of bands (hexane solution).
[d] KBr pellet.
[e] Hexane solution, the 1400–1500 cm^{-1} region not measured.
[f] Not observed in toluene solution.

TABLE 10. Comparison of the $(\mu\text{-Cl})_2Mg[Cp'(O_{Ether})]$ moiety in **2D**, **3D**, $(\eta^5\text{-}C_5H_5)MgCl(OEt_2)]_2$ **(I)** [a] and $[(\eta^5\text{-}C_5Me_5)MgCl(OEt_2)]_2$ **(II)** [a]; average values for bond distances [Å] and bond angles [°]

	2D	3D	I	II
Mg(2)–Cl	2.440(5)	2.440(3)	2.430	2.443
Mg(2)–O	2.033(8)	2.021(5)	2.048(3)	2.073
Mg(2)–C(Cp)	2.35(2)	2.39(1)	2.394	2.405
Mg–Mg	3.380(4)	3.373(2)	3.43	3.52
Cl–Mg(2)–Cl	87.6(2)	88.0(1)	90.10(5)	87.6
Mg(1)–Cl–Mg(2)	89.7(2)	89.6(1)	89.90(5)	92.4

[a] Reference [22].

2D (C(111) 0.01 Å, C(211) 0.06 Å) and **3D** (C(111) 0.10 Å, C(211) 0.03 Å) shows the absence of steric repulsion between them and other ligands.

Compound **1C** was found to be unusually thermally stable up to 170°C in xylene solution. It decomposed in a non-uniform way at 200°C. Surprisingly enough, **1C** did not show any stoichiometric reaction with the less sterically hindered, compared to BTMSA, diphenylacetylene (DPA) up to 100°C. The substitution of BTMSA by DPA is known to proceed smoothly in **1B** [9]. Instead, a slow cyclotrimerization of DPA was observed at the room temperature on the time scale of weeks, more rapidly at 100°C. Even in the latter case **1C** remained unchanged and its catalytic activity in the cyclotrimerization of DPA was preserved. The reactivity of **1C** towards terminal acetylenes is under study.

Acknowledgments

The authors thank Dr. V. Hanuš and Dr. M. Polášek for mass spectrometric analysis, Dr. P. Sedmera for NMR and G. Dörfner for EDX measurements. This investigation was supported by the Grant Agency of the Czech Republic (Grant No. 203/93/0143), by the Grant Agency of the Academy of Sciences of the Czech Republic (Grant No. 44014) and by the Fonds der Chemischen Industrie, G.S. dankt der Studienstiftung des Deutschen Volkes für ein Doktorandenstipendium.

References and notes

1 W. Beck, B. Niemer and M. Wieser, *Angew. Chem., Int. Ed. Engl., 32* (1993) 923.
2 D.M. Hoffman, R. Hoffmann and C.R. Fisel, *J. Am. Chem. Soc., 104* (1982) 3858.
3 V. Varga, K. Mach, G. Schmid and U. Thewalt, *J. Organomet. Chem., 454* (1993) C1.
4 K. Mach and J.B. Raynor, *J. Chem. Soc., Dalton Trans.,* (1992) 683.
5 T. Vondrák, K. Mach and V. Varga, *Organometallics, 11* (1992) 2030.
6 S.I. Troyanov, K. Mach and V. Varga, *Organometallics, 12* (1993) 3387, and references therein.
7 H. Antropiusová, A. Dosedlová, V. Hanuš and K. Mach, *Transition Met. Chem., 6* (1981) 90.
8 K.C. Ott, E.J.M. deBoer and R.H. Grubbs, *Organometallics, 3* (1984) 223.
9 V.V. Burlakov, U. Rosenthal, P.V. Petrovskii, V.B. Shur and M.E. Vol'pin, *Metalloorg. Khim., 1* (1988) 953.
10 V. Varga, K. Mach, M. Poláček, P. Sedmera, J. Hiller, U. Thewalt and S.I. Troyanov, *Organometallics*, submitted.
11 F. Calderazzo, F. Marchetti, G. Pampaloni, W. Hiller, H. Antropiusová and K. Mach, *Chem. Ber., 122* (1989) 2229.
12 R. Brüggemann, T. Debaerdemaeker, B. Müller, G. Schmid and U. Thewalt, ULM-Programm-system (1. Jahrestagung der Deutschen Gesellschaft für Kristallografie, Mainz, 9–12. June 1992, Preprint of *Suppl. 5, Zeitschrift für Kristallografie*, p. 33.)
13 Further details concerning the crystal structure analyses are available upon request from the Fachinfomationszentrum Karlsruhe, Gesellschaft für wissenschaftlich-technische Information mbH, D-76012 Karlsruhe by quoting the deposition number CSD-57509, the names of the authors and the journal citation.
14 G. Schmid, U. Thewalt, S.I. Troyanov and K. Mach, *J. Organomet. Chem., 453* (1993) 185.
15 J.D. Zeinstra and J.L. De Boer, *J. Organomet. Chem., 54* (1973) 207.
16 L.M. Engelhardt, R.I. Papasergio, C.L. Raston and A.H. White, *Organometallics, 3* (1984) 18.
17 W. Bünder and E. Weiss, *J. Organomet. Chem., 92* (1975) 1.
18 V.V. Burlakov, U. Rosenthal, R. Beckhaus, A.V. Polyakov, Z.T. Struchkov, G. Oehme, V.B. Shur and M.E. Vol'pin, *Metalloorg. Khim., 3* (1990) 476.
19 H. Kriegsmann and H. Beyer, *Z. anorg. allgem. Chem., 311* (1961) 180.
20 M.I. Al-Hassan, I.M. Al-Najjar and I.M. Al-Oraify, *Magn. Resonance. Chem., 27* (1989) 1112.
21 U. Rosenthal, G. Oehme, V.V. Burlakov, P.V. Petrovskii, V.B. Shur and M.E. Vol'pin, *J. Organomet. Chem., 391* (1990) 119.
22 C. Dohmeiner, D. Loos, C. Robl, H. Schnöckel and D. Fenske, *J. Organomet. Chem., 448* (1993) 5.